Three Dimensional In Vitro *Tumor* Platforms for Cancer Discovery

Manasa Gadde, Dan Marrinan, Rhys J. Michna, and Marissa Nichole Rylander

Abstract Traditional experimental platforms to study cancer biology consist of two-dimensional (2D) cell culture systems and animal models. Although 2D cell cultures have yielded fundamental insights into cancer biology, they do not provide a physiologically representative three-dimensional (3D) volume for cell attachment and infiltration. These systems also cannot recapitulate critical features of the tumor microenvironment including hemodynamics, matrix mechanics, cellular crosstalk, and matrix interactions in a dynamic manner, or impose chemical and mechanical gradients. While animal models provide physiologic fidelity, they can be highly variable and cost prohibitive for extensive biological investigation and therapeutic optimization. Furthermore, the interplay of many different microenvironmental variables, such as growth factors, immune reaction, and stromal interactions, make it difficult to isolate the effect of a specific stimulus on cell response using animal models. Due to these limitations, 3D in vitro tumor models have recently emerged as valuable tools for the study of cancer progression as these systems have the ability to overcome many of the limitations of static 2D monolayers and mammalian systems. Initial 3D in vitro models have consisted of static 3D co-culture platforms and have been successful in providing a deeper insight compared to animal and static 2D systems. However, the majority of these existing systems lack the presence of physiological flow, a pivotal stimuli in tumor growth and metastasis and

M. Gadde
Department of Biomedical Engineering, The University of Texas at Austin, Austin, TX 78712, USA
e-mail: mgadde@utexas.edu

D. Marrinan • R.J. Michna
Department of Mechanical Engineering, The University of Texas at Austin, Austin, TX 78712, USA
e-mail: dan.marrinan@gmail.com; michnarhys@utexas.edu

M.N. Rylander (✉)
Department of Biomedical Engineering, The University of Texas at Austin, Austin, TX 78712, USA

Department of Mechanical Engineering, The University of Texas at Austin, Austin, TX 78712, USA
e-mail: mnr@austin.utexas.edu

S. Soker, A. Skardal (eds.), *Tumor Organoids*, Cancer Drug Discovery and Development, DOI 10.1007/978-3-319-60511-1_5

important consideration for transport of diagnostic or therapeutic agents. In order to consider the influence of flow on cancer progression microfluidic platforms are being widely used. The integration of microfluidic technology and microfabrication techniques with tumor biology has resulted in complex 3D microfluidic platforms capable of investigating various key stages in cancer evolution including angiogenesis and metastasis. 3D microfluidic platforms are able to provide a physiologically representative tumor environment while allowing for dynamic monitoring and simultaneous control of multiple factors such as cellular and extracellular matrix composition, fluid velocity and wall shear stress, and both biochemical and mechanical gradients.

Keywords Collagen type I • Tumor platform • Tumor microenvironment • 3D model • Microfluidics • Angiogenesis • Sprouting • Endothelial • 3D cell culture • In vitro • Tumor model

1 Collagen Characterization for the Use of Tumor Platform

It is well known that three dimensional (3D) cell culture platforms have numerous advantages over their two dimensional (2D) cell monolayer counterparts, as they more accurately represent the tumor environment in vivo [1–4]. Extracellular matrix (ECM) protein collagen I, sourced from tissue, has been widely used for 3D tissue engineering scaffolds and cell culture materials due to its capacity to promote cell adhesion, growth, and proliferation [5–11]. However, challenges arise when collagen hydrogels are used to mimic specific native tissue and ECM properties. Traditionally, gels fabricated from collagen type I for tissue engineering scaffolds possess highly variable material properties as compared to synthetic ECM materials, with these properties being dependent on a number of fabrication parameters [7, 12–14]. Tight control over a broad range of parameters such as collagen source, method of solubilization, polymerization pH and temperature, ionic strength, and concentration of collagen could result in consistently reproducible hydrogel properties. However, the relationship between each of the key fabrication parameters and the functional properties (e.g. matrix stiffness, pore size, fiber structure) of these platforms have not been thoroughly investigated to sufficiently establish a robust methodology for creating platforms that mimic specific tissue microenvironments. These properties and methods for their characterization have been reviewed by the Rylander group [15]. Figure 1 summarizes the wide variability in the distribution of collagen sourcing, collagen extraction methods, and stock collagen concentrations that result from various isolation techniques. Collagen concentrations in the range of 1–5 mg/mL are most commonly used, however, these concentrations are lower than the collagen content of many native tissues [16, 17]. Many types of disease, particularly cancer, can be described using relationships between tissue elasticity and cell response where increased matrix stiffness, together with greater collagen content, is a common trait of many tumors [31, 18, 19].

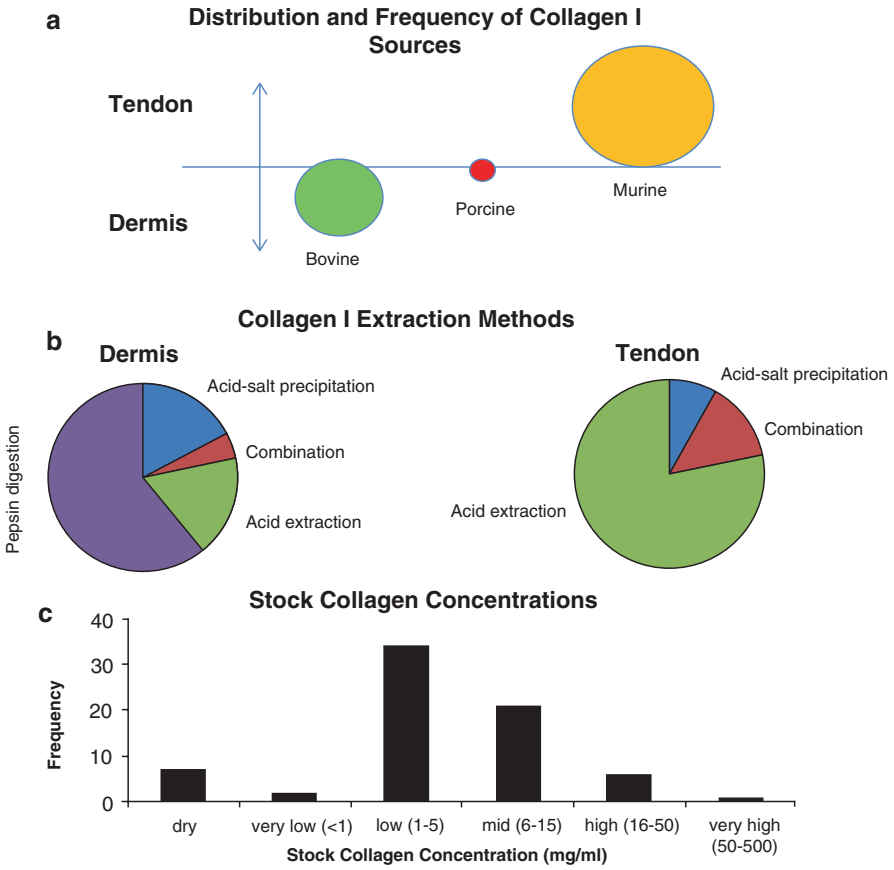

Fig. 1 Synopsis of collagen I sources and solubilization methods. (**a**) Source tissue compared with source animal; (**b**) extraction methods as compared with source tissue; (**c**) collagen concentraton in stock solutions [15]

Other factors that influence hydrogel properties are polymerization temperature and pH at which self-assembly of collagen molecules occurs. Polymerization at high temperatures results in less-ordered structures while low-temperatures create desirable pore sizes for cell proliferation [18, 19]. Elevating pH has been shown to increase collagen gel modulus but there is a decrease in cell viability outside the pH range of 7.4–8.4 [11, 22–26]. Figure 2 shows a summary of established relationships, correlating fabrication parameters and material properties [15]. This figure shows the apparent complexity and breadth of fabrication-property relationships, and it demonstrates the areas where relationships are unknown/unclear/contradictory and need further investigation and characterization. Specifically, the relationships between polymerization temperature and several mechanical properties (compression modulus, tension modulus, shear modulus) and between collagen concentration and fiber diameter require more exploration.

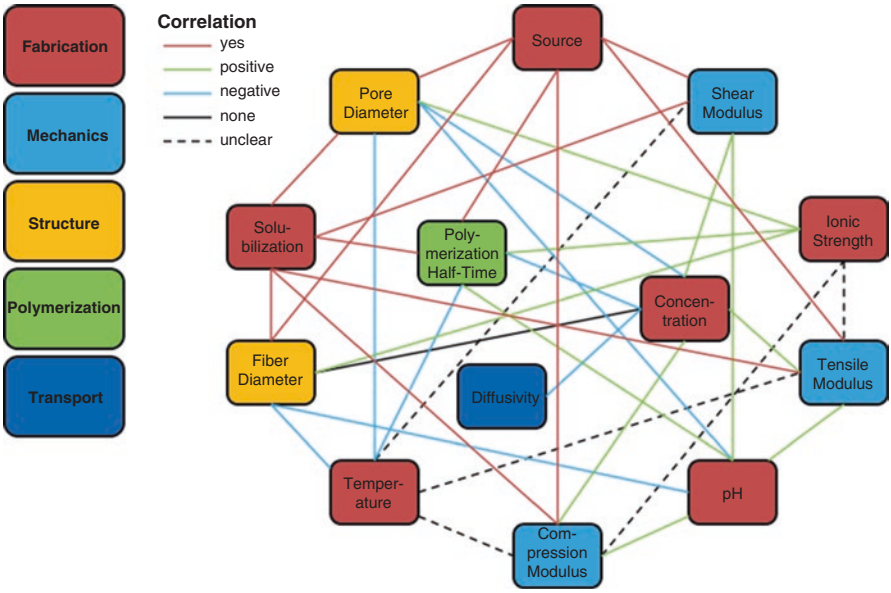

Fig. 2 Correlation between fabrication parameters and material properties for collagen hydrogels [15]

Fiber structure and scaffold stiffness are significant features of engineered cell 3D constructs, as they influence cell membrane stiffness, adhesion, differentiation, morphology, and migration [10, 11, 21, 27–35]. Because of the range of collagen hydrogel fabrication protocols, uniform characterization methods and reproducible material characteristics are needed to create predictable tissue models. In the literature, there is generally poor agreement among quantitative mechanical measurements due to differences in hydrogel fabrication parameters. The Rylander group has extensively characterized collagen type I hydrogels, correlating physiological material and transport properties (stiffness, pore and fiber diameter, diffusivity) and fabrication parameters with the intent of designing hydrogels with matching properties of target tissues. The fabrication parameters that were varied in this study were: (1) collagen concentration, (2) polymerization temperature, and (3) polymerization pH. To study the transport properties of collagen hydrogels, fluorescently tagged dextran of varying hydrodynamic radii comparable to cytokines and other bioactive molecules were used [36].

As one would expect, increased collagen concentration resulted in faster initiation of polymerization but there were no significant relationships between polymerization kinetics and pH. With regard to mechanical properties, experiments showed an increased compression modulus with all three fabrication parameters as shown in Fig. 3a. Hydrogels polymerized at low temperature (Fig. 3b:a, b) exhibited more

Fig. 3 (continued) (**c**) Pore and fiber diameter of collagen hydrogels in relation to fabrication parameters: polymerization pH, polymerization temperature, and absolute collagen concentration. *Blue* markers with dashed lines represent hydrogels polymerized at 23 °C while *red* markers with *solid lines* represent hydrogels polymerized at 37 °C. Data shown are mean + SE with N = 12. Significance was calculated for pH-averaged groups. At each concentration, the difference between means at T-23 °C and T = 37 °C is significant at $p < 0.0001$ for both fiber diameter and pore diameter [36]

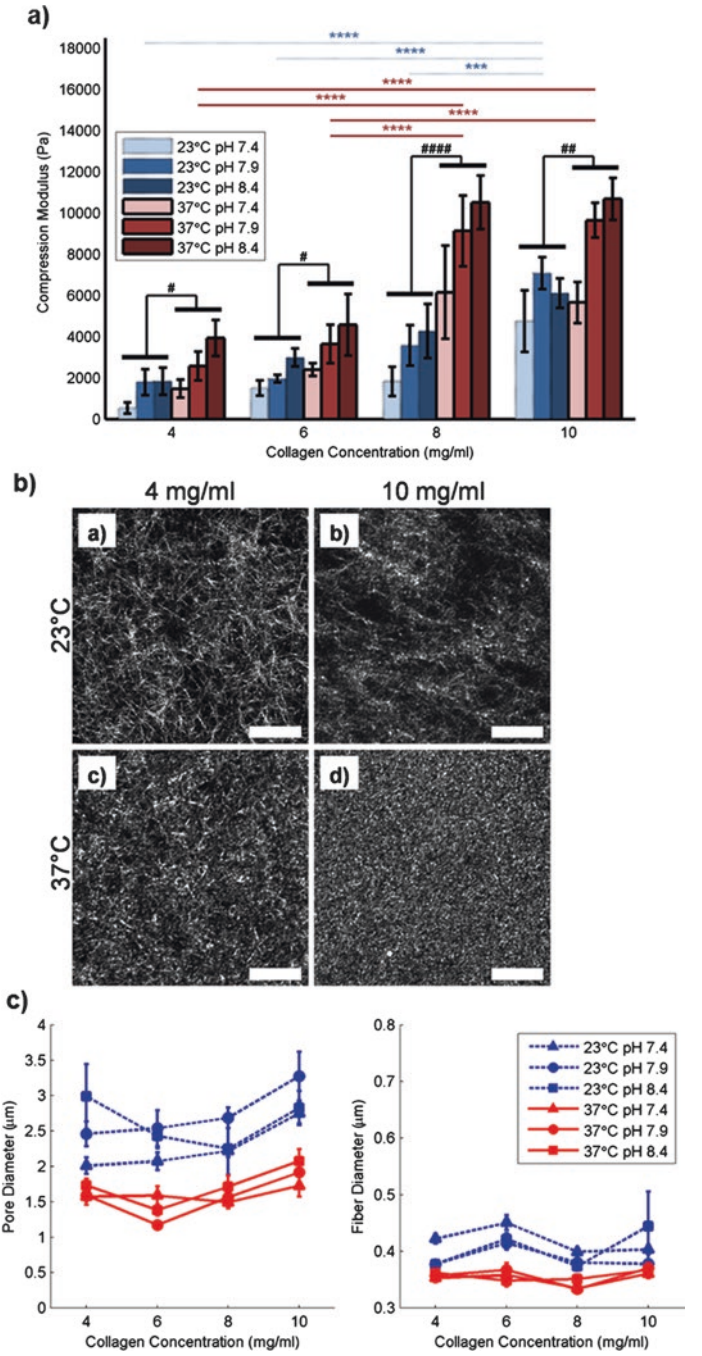

Fig. 3 (**a**) Compression moduli of collagen I hydrogels at deformation rate of 0.1%/s. *Blue bars* with *dashed lines* indicate hydrogels polymerized at 23 °C, and *red bars* with *solid lines* indicate hydrogels polymerized at 37 °C. pH is depicted as color saturation. Data shown are mean + SE with N = 4–16 per bar. Significance was calculated for pH-averaged groups (N = 12–48) as indicated by horizontal black bars. Temperature means comparison is indicated with # while hydrodynamic radius means comparison is indicated with *. (**b**) Fiber structure images obtained using confocal reflectance microscopy. Images shown are for hydrogels polymerized at pH 7.4. Scale bar is 25 μm.

network-like structures while high temperature polymerized hydrogels (Fig. 3b:c, d) resulted in evenly distributed fibers with decreased mesh size. All variations of fabrication parameters and the effects on fiber structure are summarized in Fig. 3c. Diffusivity was largely influenced by hydrodynamic radii of diffusing molecules, with the effects of fabrication parameters made negligible compared to sizes of fluorescent dextran molecules. This study not only illuminated relationships between fabrication parameters and collagen material properties, but these relationships were also used to generate a set of empirical equations that could be applied when designing and optimizing tissue models as shown in Table 1 [36].

2 3D In Vitro Collagen Tumor Models

2D cell monolayers are unable to truly recapitulate the dynamic tumor microenvironment (TME), as they do not incorporate accurate architectural features and critical cell-cell and cell-matrix interactions [37–41]. 3D cell culture models have provided significant insight regarding the role of the TME on tumor growth and development [17, 42–48]. Fischbach, *et al.* have established a number of 3D in vitro tumor models using both native and synthetic polymeric materials for tissue scaffolds [17, 42, 48]. These tumor constructs have shown angiogenic growth factor secretion and drug responsiveness, effects of oxygen tension within tumors and 3D cell-ECM interactions on angiogenic potential, and remodeling of collagen type I ECM by endothelial cells in response to release of angiogenic factors from cancer cells.

A bioengineered collagen type I tumor model developed by the Rylander group is representative of the pre-vascularized stage of solid tumor progression [49]. This stage of tumor growth is characterized by altered TME properties such as uninhibited proliferation, a necrotic core surrounded by hypoxic regions, and activation of genetic factors that lead to the recruitment of local endothelial cells for promoting angiogenesis [50–53]. Hypoxia, an oxygen deficient environment, occurs at a distance of 100 to 200 μm from the nearest vessel. Cells in the core of a growing tumor mass that cannot adapt to hypoxic conditions begin to undergo apoptosis, forming a necrotic core as shown in Fig. 4a. Hypoxia-inducible factor (HIF)-1α is a key marker for hypoxia [50, 53]; HIF-1α is a heterodimeric transcription factor that is protected from degradation when hypoxic levels are reached in the surrounding tissue. Tumors react to the altered hypoxic stress in the TME by progressing from a pre-vascularized to a vascularized state, inducing an angiogenic response. During this progression, tumor cells secrete cytokines and growth factors (e.g. vascular endothelial growth factor A, VEGF-A) that stimulate vascular sprouting and neovascularization from proximate endothelial cells [54].

In the bioengineered collagen type I tumor model developed by the Rylander group described in the previous paragraph, MDA-MB-231 breast cancer cells were seeded in collagen type I (8 mg/mL) hydrogel constructs for 7 days as shown in Fig. 4b. By day 3 in culture in the hydrogels, cells developed a stellate, elongated morphology with disorganized nuclei, and by day 7, cells proliferated and aggregated into 3D clusters, exhibiting cell-cell and cell matrix interactions representative

Table 1 Shows the sensitivity of significant hydrogel properties to fabrication parameters

Polymerization half-time ($R^2 = 0.565$)				Compression modulus ($R^2 = 0.504$)				Pore diameter ($R^2 = 0.332$)				Diffusivity ($R^2 = 0.867$)				
	C	T	pH		C	T	pH		C	T	pH		C	T	pH	r_H^{-1}
C	–0.78	0.79	–	C	1	–	–	C	0.40	–	–	C	–0.11	–	–	–
T	0.79	–1	–	T	–	0.48	–	T	–	–1	–	T	–	–0.002	–	–
pH	–	–	–	pH	–	–	0.39	pH	–	–	0.27	pH	–	–	–0.03	0.37
												r_H^{-1}	–	–	0.37	1

C concentration in mg/mL, *T* temperature in °C, and r_H hydrodynamic radius in nm

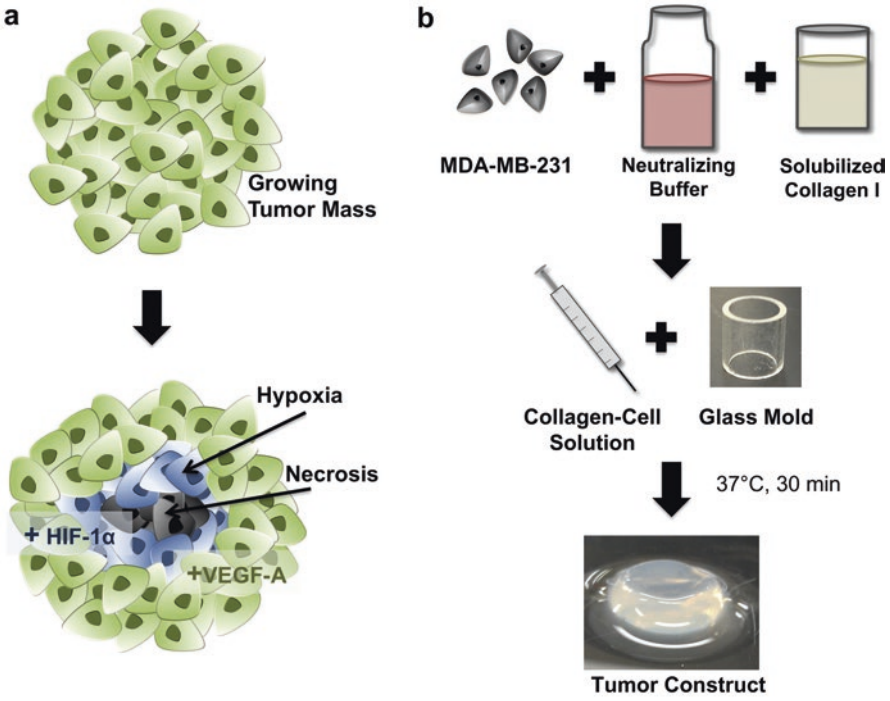

Fig. 4 (**a**) Regions of hypoxia surrounding a necrotic core, as a result of uninhibited proliferation of tumor cells during pre-vascularized stages of in vitro solid tumor development. (**b**) Bioengineered in vitro solid tumor platform consisting of collagen I hydrogels cultured with MBA-MB-231 human breast cancer cells [49]

of in vivo behavior [49]. Cell seeding density (1 or 4 million cells/mL) and scaffold thickness (1.5 or 3 mm) were varied with the intent to promote the development of hypoxia and necrosis via diffusion limitations for oxygen and nutrients. Figure 5 shows the effects of cell seeding density on the nutrient and oxygen availability at depths greater than 150 to 200 μm from the surface of the hydrogels, where cells are in direct contact with oxygenated media. In the hydrogels with 4 million cells/mL density, large amounts of dead cells (stained with propidium iodide) were present at this depth, followed by a space containing no visible cells. The complete absence of cells in this void could be due to cells migrating to the outer boundary to be in closer proximity to oxygen and nutrients. Alternatively, since propidium iodide is a nuclear stain, the void could be indicative of DNA degradation in dead cells nearest the center [55].

To demonstrate that hypoxia is an identifiable precursor to cell death, high-density cell constructs (4 million cell/mL in 3 mm thick hydrogels) were used to induce formation of a necrotic core. Immunofluorescence imaging of HIF-1α was performed to assess intracellular levels of hypoxia. HIF-1α was detected on day 1 with increasing intensity by day 5, attributed to tumor cell proliferation and the subsequent increase in competition for oxygen. It is assumed that cell access to oxygen and nutrients in confined 3D constructs is more difficult than 2D cell monolayers.

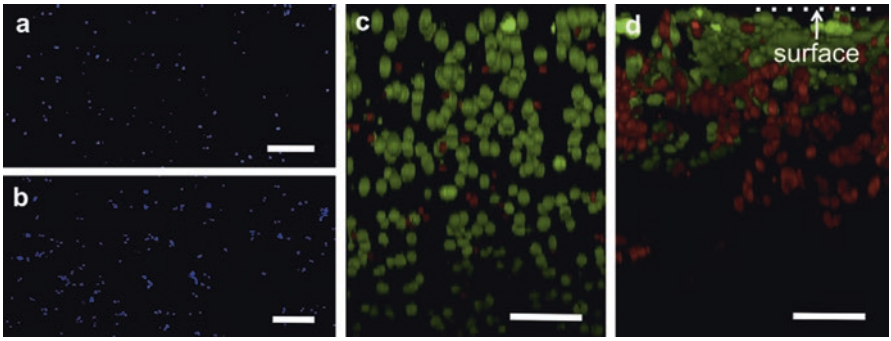

Fig. 5 (**a**) Day 1 of MDA-MB-231 cells that were seeded at 1 million cells/ml in collagen hydrogels. Cells were evenly distributed throughout the hydrogel. (**b**) On day 5, cells show significant proliferation and formation of 3D clusters. (**c**) Cell seeding density was increased to 4 million cells/ml, and on day 1, viable cells (*green*) were evenly distributed throughout the gel with few dead cells (*red*). (**d**) On day 5, the higher-density cell constructs showed viability through 150–200 μm depth below the surface, with limiations in oxygen and nutrients resulting in cell death toward the core of the bioengineered tumor platforms. Scale bars are 250 μm (**a, b**) and 100 μm (**c, d**) ([49])

Therefore, measurable amounts of HIF-1α on day 1 confirm the hypoxic cell reaction to being cultured in 3D. When cells were seeded in 3 mm thick constructs containing 4 million cells/mL, HIF-1α gene expression, analyzed using quantitative RT-PCR, was upregulated on days 3 and 5. By day 7, there was a decrease in HIF-1α expression, attributed to hypoxic cells dying from deficient oxygen and nutrient availability. VEGF-A expression was upregulated on days 3, 5, and 7 compared to day 0, but expression decreased between days 5 and 7. This decrease was likely an effect of down regulation of HIF-1α observed on day 7. When cells were seeded in 3 mm thick constructs at a lower density of 1 million cells/mL, the competition for nutrients and oxygen was alleviated. This led to an initial down regulation of HIF-1α and eventual upregulation of VEGF-A. Expression of HIF-1α was upregulated on days 3 and 5 compared to day 1, and on day 7 compared to day 0. Both HIF-1α and VEGF-A gene expression peaked at day 5 in the high-density (4 million cells/mL) constructs, but in the low-density (1 million cells/mL) constructs, constant upregulation of both markers was observed over the 7-day period [49]. Increased VEGF-A expression is a strong indicator of angiogenic potential in tumors, and a key aspect of tumor maturation is VEGF-A inducement of endothelial cells to promote tumor vascularization [54, 56]. After decreasing scaffold thickness to 1.5 mm while maintaining high-density cell seeding of 4 million cells/mL, no significant upregulation of either HIF-1α or VEGF-A was detected on any day compared to day 0. The reduced thickness diminished diffusion limitations of oxygen and nutrients. This 3D bioengineered tumor model was representative of the pre-vascularized stage of solid tumor progression, and led to the development of multilayered, co-cultured tumor constructs demonstrating the angiogenic and neovascularization processes when cancer cells interacted with endothelial cells [57].

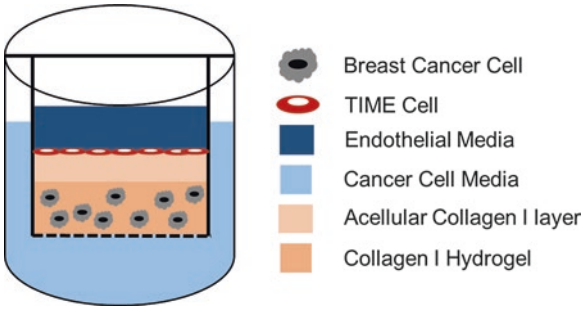

Fig. 6 Bilayer collagen type I hydrogel composed of a collagen type I hydrogel with breast cancer cells on the bottom and an acellular collagen type I hydrogel seeded with TIME cells on top. The bilayer collagen type I hydrogel is housed in a transwell system

The Rylander group has also developed a 3D bilayer vascular tumor platform to investigate the importance of matrix properties, cell-cell interactions, and growth factors on promoting and supporting angiogenesis [57]. The tumor platform is a bilayer collagen type I hydrogel in which the bottom layer is composed of 8 mg/mL collagen type I seeded with MDA-MB-231 (highly aggressive) or MCF7 (less aggressive) breast cancer cells. The top layer of the platform is an acellular hydrogel composed of collagen type I with telomerase immortalized endothelial (TIME) cells seeded on top as shown in Fig. 6. The acellular region in the bilayer hydrogel was deemed necessary by preliminary studies which showed direct contact between tumor and endothelial cells lead to apoptosis of endothelial cells [58–60]. The bilayer collagen hydrogel was housed in a transwell system allowing for separation of media components for the various cell types and ensures TIME cells from being exposed to the acidic metabolites and wastes generated by the MDA-MB-231 or MCF7 cells. The following parameters in Table 2 were varied by the Rylander group to determine the cellular and matrix properties that influence angiogenesis in a co-culture of TIME and breast cancer cells.

To determine if tumor cells could elicit an angiogenic response from the TIME cells without any exogenous growth factors, TIME cells were grown in 3D bilayer tumor platforms with either MDA-MB-231 or MCF7 cells on either 2, 4, or 8 mg/mL acellular collagen layers as illustrated in Fig. 6. To remove the influence of exogenous growth factors, TIME cells were cultured in endothelial growth media (EGM) that did not include traditional supplements of vascular endothelial growth factor (VEGF) and basic fibroblast growth factor (bFGF) (promoters of angiogenesis). In both co-culture groups, TIME cells displayed an elongated and aligned morphology and the MDA-MB-231 and TIME co-culture also resulted in an increase in endothelial proliferation with confluence reached by day 7. Conversely, MCF7 co-cultures led to a decrease in endothelial proliferation and confluence of TIME cells was not achieved. This behavior is supported by preliminary studies performed by the Rylander group consisting of MDA-MB-231 and MCF7 monocultures grown in collagen type I hydrogels. The results from preliminary studies revealed that from day 1, MDA-MB-231 cells produced VEGF levels much higher than 2 ng/mL present in complete EGM whereas MCF7 cultures required 5 days to produce the amount of VEGF similar to that found in EGM. The increased endothelial proliferation can be attributed to the high levels of VEGF produced by the

Table 2 Details of the various parameters that were investigated for their influence on inducing an angiogenic response

Experimental parameters for testing angiogenic response			
	MDA-Mb-231	MCF7	
Tumor cell density	1×10^6 cells/mL	5×10^6 cells/mL	
TIME cell density	3×10^4	1×10^5	
Acellular collagen type I concentration	2 mg/mL	4 mg/mL	8 mg/mL
Growth factors	EGM with VEGF and bFGF removed	Complete EGM (2 ng/mL VEGF, 4 ng/mL bfGF)	EGM with 10 ng/mL bFGF
Time of TIME cell seeding	1 day into culture	5 days into culture	

MDA-MB-231 cells from the beginning which prompted their proliferation whereas MCF7 cells were unable to produce necessary levels of VEGF at an early time point necessary for the growth of the TIME cells. Additionally, these results were consistent in all three concentrations of acellular collagen layers suggesting that endothelial morphology is influenced by tumor-endothelial interactions but endothelial proliferation is most influenced by the presence of VEGF.

Angiogenic sprouting was studied in bilayer co-cultures of TIME cells with either MDA-MB-231 or MCF7 cells, and in bilayer monoculture of TIME cells with TIME cells grown on a 2, 4, or 8 mg/mL acellular collagen layer. Sprouting of TIME cells was observed on the 2 and 4 mg/mL acellular collagen layers in MDA-MB-231 and TIME co-culture and in the TIME monoculture but not in the MCF7 co-culture with sprouting more prominent on the 2 mg/mL acellular collagen layers. MDA-MB-231 and TIME co-culture produced capillary like tubule networks that penetrated into the acellular collagen, while TIME monoculture showed no signs of tubule formation beneath the surface revealing a connection between matrix concentration (stiffness), presence of tumor cells (aggressive vs non aggressive), and angiogenic sprouting (invasive vs not invasive).

To further elucidate the angiogenic response of tumors, correlation between angiogenic sprouting and growth factors bFGF and VEGF was investigated by altering media composition and initial seeding density of MDA-MB-231 cells. Following the results from the previous experiment, TIME cells were cultured on either 2 or 4 mg/mL acellular collagen as these levels were capable of inducing sprouting. To determine if MDA-MB-231 cells can induce sprouting without exogenous growth factors, TIME cells were cultured in either complete EGM (2 ng/mL VEGF and 4 ng/mL bFGF), complete EGM supplemented with additional bFGF (2 ng/mL VEGF and 10 ng/mL bFGF), or EGM without the addition of VEGF and bFGF supplements. MDA-MB-231 and TIME co-cultures grown in EGM with bFGF and VEGF present showed enhanced angiogenic sprouting compared to media with exogenous growth factors lacking as presented in Fig. 7. Increasing bFGF levels from 4 to 10 ng/mL did not increase sprouting and this behavior persisted regardless of the initial seeding density of MDA-MB-231 cells (1 vs 5 million MDA-MB-231 cells). Even

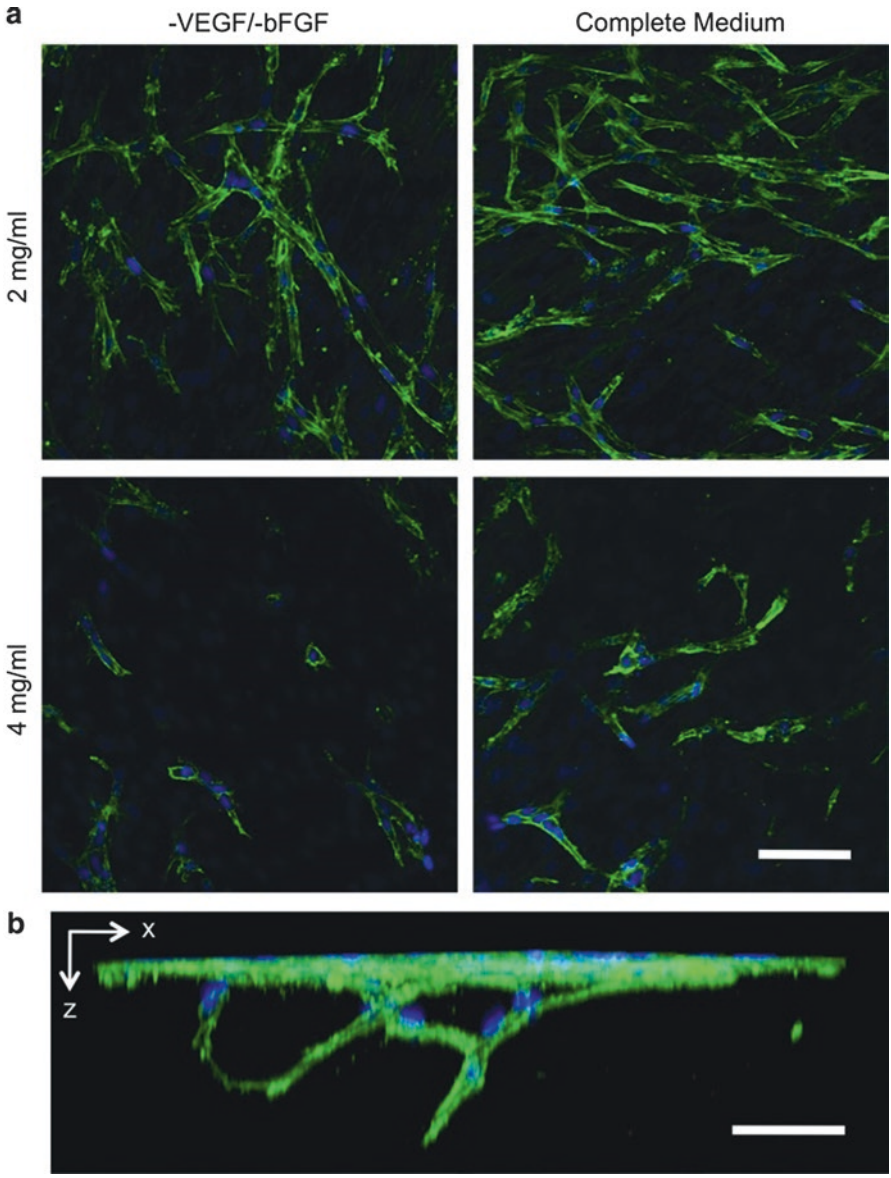

Fig. 7 Influence of matrix concentration and supplemented bFGF on angiogenic sprouting of TIME cells cultured for 7 days on MDA-MB-231 bioengineered tumors. (**a**) Greater degree of angiogenic sprouting was observed within the 2 mg/mL acellular collagen layers as compared with the 4 mg/mL acellular collagen with augmented sprouting in both 2 and 4 mg/mL in the presence of media containing bFGF. (**b**) Three-dimensional image reconstruction shows two separate tubules anastomosing and extending down beneath the surface monolayer (2 mg/mL acellular collagen layer; 10 ng/mL bFGF). *Green*, F-actin; *blue*, nuclei. Scale bars are 50 μm [57]

when exogenous VEGF component was not present in EGM, VEGF wasn't completely absent from the system due to the presence of endogenous VEGF produced by MDA-MB-231 cells. Results revealed that VEGF had an influence on endothelial proliferation and presence of both bFGF and VEGF is necessary for a complete angiogenic response agreeing with previous studies that showed that co-stimulation of bFGF and VEGF augmented angiogenic sprouting in an endothelial monoculture assay [61].

Finally, the Rylander group investigated the influence of TIME cells on angiogenic response by comparing two different seeding densities of TIME cells: low (3×10^4) and high (1×10^5, equivalent to a confluent monolayer). Using the optimal sprouting conditions determined from previous bilayer collage type I hydrogel experiments (MDA-MB-231 co-culture, 2 mg/mL acellular collagen layer, initial MDA-MB-231 seeding density of 1 million cells) they observed that increasing the initial density of TIME cells resulted in an increase in the number of sprouts but the presence of tubule networks occurred at the same time point of 5 days into co-culture regardless of the seeding density. Additionally, the time at which TIME cells were introduced to the co-culture, day 1 vs day 5 (time point at which MDA-MB-231 cells secrete high levels of VEGF), did not increase the rate of tubule formation which once again was observed 5 days into co-culture. These results illustrated that along with necessary levels of VEGF and appropriate matrix concentration, a time dependent tumor-endothelial interaction is necessary for tubule formation. The 3D in vitro vascularized tumor-endothelial co-culture model developed by the Rylander group revealed that the type of tumor cells present, cell-cell interactions, seeding density, matrix concentration, and growth factors are all involved in eliciting an angiogenic response, and it is important to use a system that allows for the presence of all these factors to understand the complexity of tumor developments.

3 Microfluidic Vascularized Tumor Platform

Microfluidic technology was introduced as an analysis tool for biology and chemistry in the early 1990s [62]. It is the manipulation of micro scale volumes of fluids in a microchannel system with dimensions that range from 1 to 1000 μm [63, 64]. The combination of microfluidic technology with cancer biology and drug delivery has enabled development of complex 3D tumor models that provide a more controllable environment while allowing researchers to isolate specific interactions that are absent in 2D models and difficult in animal models [65]. 3D microfluidic platforms are able to recapitulate the complex cell-cell and cell-ECM interactions within dynamic microenvironments characterized by controllable spatial cell distribution and tunable gradients of biochemical and biophysical factors [66].

Microfluidic tumor platforms have a number of advantages over existing tumor models. They use small quantities of cells and reagents and are able to perform experiments with short processing times yielding high resolution and sensitivity [63, 67]. Incorporation of microfabrication techniques has led to development of

physiologically relevant TMEs with tissue properties present in vivo such as crosstalk between cells and their microenvironment, vascularization, perfusion, and formation of gradients in nutrients, oxygen, and other soluble factors [68]. Mass transport in microfluidic technology is governed by diffusion due to the small scale resulting in precise spatial and temporal control over gradients of soluble biological factors and cell-cell and cell-ECM interactions. This allows for formation of gradients and the retentions of molecules such as signaling factors and nutrients, in close proximity to cells increasing response sensitivity. Additionally, controlled fluid flow through microchannels simulates the vascular system and interstitial flow and provides constant culture medium refreshment for prolonged culture [65, 69]. Other advantages of 3D microfluidic platforms are that they can mimic important mechanical and biochemical parameters including hypoxia, increased pressure, and shear stress [67, 68]. Finally, multiple microfluidic devices can be connected to form an integrated multi organ platform that allows for a more comprehensive understanding of tumor behavior [70]. These benefits of 3D in vitro microfluidic platforms have resulted in their emergence as powerful systems for gaining a better understanding of cancer progression and development of new therapies.

Dr. Rylander's group has developed an optically clear collagen-based microfluidic vascularized tumor platform that recreates the cancer microenvironment and cellular crosstalk through the incorporation of an endothelialized microchannel within a collagen 3D matrix containing human cancer cells. Their previous studies utilized a 3D in vitro vascularized tumor-endothelial co-culture model to study the influence of paracrine signaling on angiogenesis. Results revealed that the type of tumor cells present, cell-cell interactions, seeding density, matrix concentration, and growth factors are all involved in eliciting an angiogenic response, and it is important to use a system that allows for the presence of all these factors to understand the complexity of tumors To gain a further understanding of cancer and its progression, additional parameters such as flow, pressure and soluble factor gradients, need to be investigated. This led to the development of the collagen-based microfluidic vascularized tumor platform. The platform, shown in Fig. 8 allows for high imaging resolution and dynamic monitoring of drug/nanoparticle transport and angiogenic vessel sprouting [71]. The microchannel is composed of collagen type I embedded with green fluorescent protein (GFP) tagged MDA-MB-231 breast cancer cells with an inner lumen of TIME cells and enclosed in fluorinated ethylene propylene (FEP) capped with polydimethylsiloxane (PDMS) sleeves. Complete details for the development of the microfluidic tumor model can be found in previous publications from the Rylander group [1, 71]. Briefly, collagen type I solution containing MDA-MB-231 cells was injected into the FEP housing with a needle placed through the center. After polymerization, the needle was removed and a solution of TIME cells was injected into the hollow lumen left behind by the needle. Next, a 72 h graded flow preconditioning treatment was applied to the microchannels exposing the TIME cells to shear stress from 0.01 to 0.1 dyn/cm^2 in order to develop a confluent endothelium as displayed in Fig. 8b, c. Once the channels are prepped, the FEP enclosure and a water bath enable refractive matching allowing for undistorted imaging of the system. This system was used to study tumor and

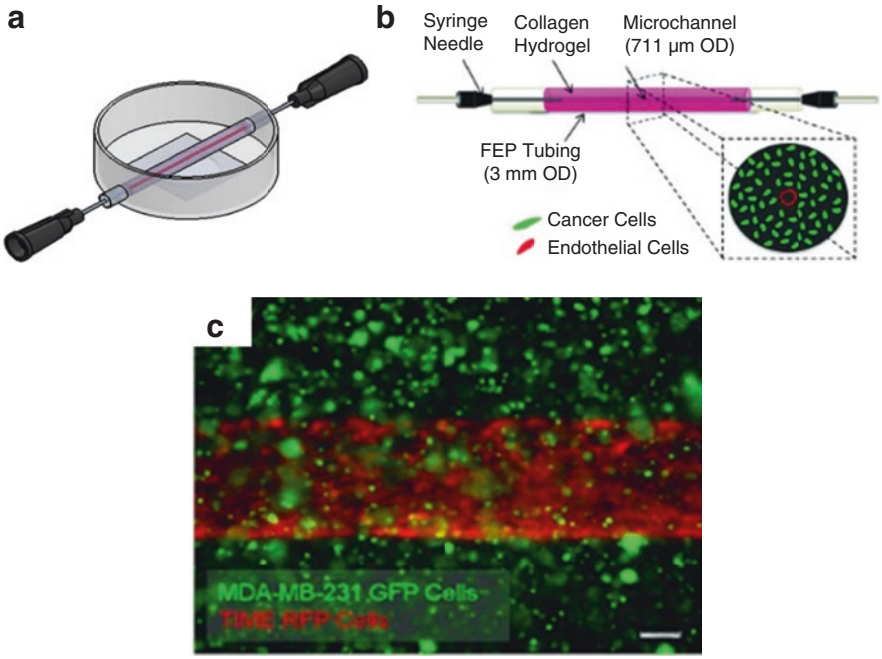

Fig. 8 Tumor-endothelial co-culture in microfluidic collagen hydrogels (**a**) Experimental setup of microfluidic vascularized tumor platform. (**b**) Schematic of a 3D microfluidic tumor vascular model in which cancer cells seeded in the bulk of hydrogel surround endothelial cells lining the lumenal surface of the central microchannel. (**c**) Co-culture maintains growth of MDA-MB-231-GFP breast cancer cells and TIME red fluorescent protein (RFP) cells within physiologically relevant geometries. Image 24 h post-culture. Scale bar is 200 μm [1]

endothelial intercellular signaling and particle transport in response to hemodynamic flow typical of the TME [1, 71, 72].

Using the collagen based microfluidic vascularized tumor model described above, the Rylander group has gained insight into the difference between intracellular signaling in mono vs co-culture and in static vs flow models. They investigated and compared the influence of mono and co-cultures of MDA-MB-231 and TIME cells in 2D tissue culture flasks and in the 3D microfluidic vascularized tumor platform exposed to either static or flow conditions. Perfusion of media through the microchannel was used to impose physical fluid shear stresses on the endothelium as well as simulate tumor-relevant hemodynamic stresses in the system, which are important for regulating reciprocal tumor-endothelial expression of angiogenic growth factors. Studies have shown that fluid shear stresses are linked to endothelial cell transcription, proliferation, barrier transport properties, and modulation of their cytoskeleton [69, 72–77] as well as stimulating and directing the migration of cancer cells [65, 78, 79]. Gene expression measured with reverse transcription polymerase chain reaction (RT-PCR) revealed that MDA-MB-231 cells cultured in static 3D microfluidic platforms compared to 2D culture had a significant increase in

expression of matrix metalloproteinase 9 (MMP9), an enzyme that degrades the ECM, as well as proangiogenic factors platelet-derived growth factor B (PDGFB) and angiopoietin 2 (ANG2). In the presence of flow, PDGFB and VEGF-A expressions were higher in comparison to 3D static conditions. Additionally, when co-cultures of MDA-MB-231 and TIME cells were studied, 3D co-culture exposed to flow showed an increased expression of proangiogenic factors of VEGF-A, ANG2, PDGFB, and MMP9 compared to 3D monocultures of MDA-MB-231 cells. In the absence of flow, only VEGFA expression was upregulated [1] These results indicate the importance of multicellular interactions in tumor platforms as well as the presence of hydrodynamic tumor vascular environment.

Subsequent published work by the Rylander group further investigated the effect of shear stress on angiogenic response and barrier function of endothelial cells [71]. They exposed the microfluidic vascularized tumor platform composed of MDA-MB-231 monoculture or co-culture of MDA-MB-231 and TIME cells to three different shear stresses, 4 dyn/cm^2 (normal microvascular wall shear stress), 1 dyn/cm^2 (low microvascular wall shear stress), and 10 dyn/cm^2 (high microvascular wall shear stress). Angiogenic response was quantified by performing PCR and ELISA for the presence of angiogenic markers such as VEGF, bFGF, and angiopoietins 1 and 2 (ANG1, ANG2). Vessel permeability was determined by perfusing the channel with fluorescent nanoparticles ranging from 20 to 1000 nm and fluorescently labeled dextran. The study revealed that the wall shear stress caused by the fluid flow down regulated angiogenic factors released by MDA-MB-231 cells in the presence of an endothelium but had no effect in the MDA-MB-231 mono-cultures as shown in Fig. 9a, suggesting that wall shear stress influences the behavior of the endothelial cells which then in turn regulate the behavior of surrounding tumor cells. Barrier function of the endothelial cells was also shown to be influenced by both the wall shear stress and the presence of tumor cells as revealed in Fig. 9b. Dextran permeability studies revealed that exposure of the endothelium in both mono and co-culture conditions to the three wall shear stresses resulted in decreasing permeability with increasing wall shear stress. Endothelial cells have been shown to elongate and align in the direction of flow and a higher shear stress can lead to the formation of a tighter and confluent endothelium [69, 74, 77]. Additionally under all three flow conditions, co-cultures of tumor and endothelial cells resulted in a leakier vessel compared to an endothelial monoculture. Previous studies have shown that contact between tumor and endothelial cells results in detachment and apoptosis of the endothelial cells [58–60]. This phenomenon combined with the paracrine signaling release of proangiogenic factors could be responsible for the increased vessel permeability in the tumor-endothelial co-culture microfluidic platform. Further permeability studies performed with fluorescently labeled dextran and 1 μm particles depicted in Fig. 10 reveal a size exclusion function of the endothelial barrier as the small dextran particle were able to easily extravasate in the collagen type I matrix whereas the 1 μm particles were too large to cross the endothelium. While the platform developed by the Rylander group has been used primarily to understand breast cancer, the platform has the ability to be employed for a variety of cancers. By tuning the ECM stiffness, composition, porosity, and using

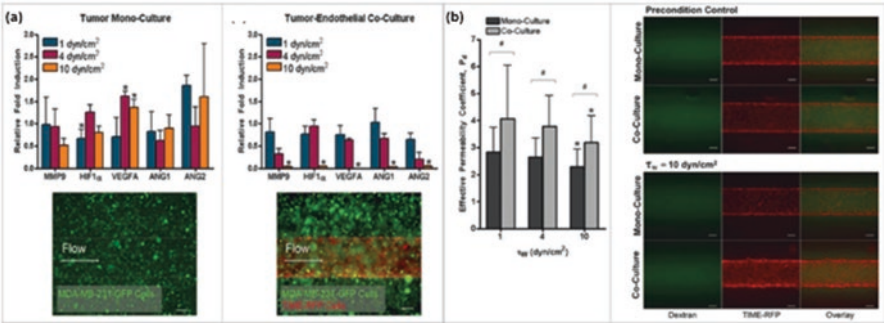

Fig. 9 Effect of wall shear stress on expression of engiogenic factors and endothelial permeability. (**a**) High wall shear stress down-regulates tumor-expressed angiogenic factors in the presence of an endothelium. Tumor mono-cultures or co-cultures with endothelial cells were cultured under the 72 h. preconditioning flow rate, after which the target wall shear stress (τ_W = 1, 4, or 10 dyn/cm^2) was introduced through the microchannel for a total 6 h. Total tumor mRNA was then isolated for gene expression analysis. Relative mRNA to GAPDH mRNA expressed as a fold induction ± standard deviation (n = 4) $^*P < 0.05$. Scale bars are 200 μm [71]. (**b**) Effective permeability coefficient, P_d, decreases as a function of increasing wall shear stress and increases during co-culture with tumor cells. P_d of 70 kDa Oregon Green-conjugated Dextran across the endothelialized microchannel decreases as τ_W increases for both mono-culture and co-culture with tumor cells, with a statistically significant reduction at τ_W = 10 dyn/cm^2 relative to the preconditioned endothelium $^*P < 0.05$. P_d during co-culture was significantly increased for all τ_W relative to mono-cultures $\#P < 0.05$. Representative images of 70 kDa Oregon Green-conjugated Dextran diffusion across the endothelialized microchannel for the case of τ_W = 10 dyn/cm^2. Scale bar is 200 μm [71]

appropriate cell types, microenvironments of desired properties can be created recapitulating cell-cell and cell-ECM interactions of different cancers by following the same preparation protocol. This model can also be easily adapted to study specific stages of tumor progression such as angiogenesis or metastasis.

In addition to the Rylander group, several other groups have developed microfluidic platforms to investigate tumor mechanisms such as angiogenesis or metastasis. Tien et al. have been developing platforms fabricated from PDMS to house layers of macromolecular hydrogels that can be stacked together to form channels incased by the hydrogel scaffold using additive methods [81]. The Beebe group used a viscous finger patterning method to create endothelialized lumen structures composed of human umbilical vein endothelial cells (HUVECs) within a collagen type I and matrigel hydrogel to study the role of VEGF and 10 T1/2 smooth muscle cells on angiogenesis [81]. They were able to create channels of various geometries with proper endothelial barrier function confirmed through permeability studies of fluorescein isothiocyanate (FITC) labeled bovine serum albumin (BSA). Using their finger patterning method, they created VEGF gradients and showed that HUVEC sprouting occurred in the direction of VEGF source and co-culture of HUVECs with 10 T1/2 cells resulted in a decrease in sprouting regardless of VEGF presence. Other groups have combined additive methods with lithographic techniques to develop in vitro microfluidic vascular networks (μVN) in a three dimensional collagen scaffold for studying angiogenesis and thrombosis [82]. μVNs seeded with

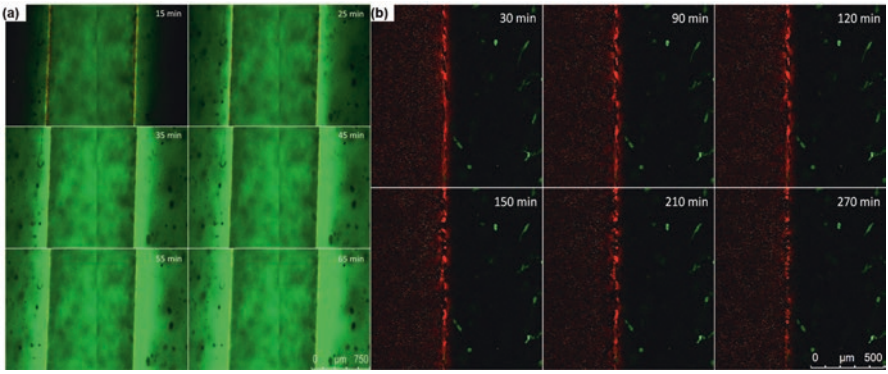

Fig. 10 Extravasation of 70 kDa Oregon Green-conjugated Dextran (**a**) and 1 μm nanoparticles from the microchannel (**b**). (**a**) Each image shows a microfluidic vascularized 3D tumor platform. The two bright *red lines* seen in the first image correspond to TIME-RFP cells that form the border between the microchannel in the *middle* of each image and the collagen surrounding it. Unlabeled MDA-MB-231 breast cancer cells are embedded in the collagen surrounding the microchannel. The *green signal* apparent in each image was produced by 70 kDa Oregon Green-conjugated Dextran. The first image corresponds to 15 min after flow containing the 70 kDa Oregon Green-conjugated Dextran was introduced to the microchannel at a flow rate corresponding to a wall shear stress of $\tau_W = 1$ dyn/ cm^2. Each corresponding image is 10 min after the previous one. As can be seen by the increase in green signal, the 70 kDa Oregon *Green*-conjugated Dextran continuously diffuses out of the microchannel through the endothelium and into the collagen for the duration of the 70 min study. (**b**) Endothelium prevents extravasation of 1 μm nanoparticles from microchannel. Each image shows half of a microfluidic vascularized 3D tumor platform. The *red signal* seen in the left half of the image was produced by 1 μm *red* fluorescent polystyrene nanospheres. The *bright red line* in the *middle* of each image corresponds to TIME-RFP cells which form a barrier between the microchannel and collagen ECM. The *green signal* seen in the right half of each image corresponds to MDA-MB-231-GFP breast cancer cells embedded within the collagen. The first image corresponds to 30 min after flow containing the 1 μm *red* fluorescent plastic nanospheres was introduced to the microchannel at a flow rate corresponding to a wall shear stress of $\tau_W = 1$ dyn/ cm^2. Each corresponding image is 60 min after the previous one. As can be seen, the 1 μm nanospheres are prevented from extravasating out of the microchannel into the collagen by the endothelium for the duration of the 6 hour study

HUVECs demonstrated appropriate endothelial morphology, intracellular junctions, and barrier function. In μVN co-cultures of HUVECs with human brain vascular pericytes (HBVPCs), half of the groups showed sprouting of HUVECs whereas the other half revealed a retracted endothelium from the walls of the microchannels. Additionally, they confirmed that their μVNs could be adapted to study thrombosis.

Another notable group in cancer microfluidics is the Kamm group who has developed multiple cancer microfluidic models to study angiogenesis and metastasis. Examples of their work include using microfluidic platforms to recreate cell-cell signaling present in bone and muscle microenvironments to investigate the metastasis of breast tumor cells to these particular organs [83]. They used 5 mg/ml fibrin gels that were embedded with primary hBM-MSCs, osteo differentiated (OD) hBM-MSCs, and HUVECs to create the bone microenvironment and for the muscle

mimic, they replaced the OD hBM MSCs with C2C12 cells. They introduced a MDA-MB-231 cell solution into a neighboring channel and observed the extravasation of the MDAs into the bone microenvironment was much higher than extravasation into the muscle microenvironment. This group has also developed a collagen type I microfluidic model embedded with endothelial cells to study the influence of transendothelial flow as a mechanical regulator of angiogenesis [84]. Endothelial cells were cultured on stiff collagen gels and subjected to no flow (control), apical-to-basal, or basal-to-apical flow for 24 hours. They found basal-to-apical transendothelial flow induced sprouting and triggered invadopodia supporting the group's hypothesis that transendothelial pressure gradients produced by basal-to-apical flow promote sprouting angiogenesis.

Other groups developing novel microfluidic platforms for cancer research include Song et al., who have designed a microfluidic vasculature system capable of site specific activation of the endothelium to model the interactions between circulating cancer cells and the endothelium during metastasis [85]. They used their microfluidic system to produce site-specific stimulation of endothelium with CXCL12, a chemokine involved in metastasis, on adhesion of circulating breast cancer cells to endothelium. Results from the study demonstrate that circulating breast cancer cells adhere to endothelium when stimulated from the basal side with CXCL12 suggesting the signaling system CXCL12-CXCR4 as a potential target for therapies aimed at blocking metastasis.

In addition to tumor platforms, microfluidic technology has been adapted to create organ level models such as those for liver and heart tissue with varying degrees of vascularization. These models were primarily developed independently and few attempts have been made to enable the interaction of all these microenvironments to study their collective influence on tumor behavior. Some microfluidic-based organ-on-a-chip systems have multiple cell culture chambers connected with microchannels [70, 86–89]. However, the cell volume in these microsystems is limited and does not allow statistically significant observations. Most of these systems are 2D and cannot truly represent the 3D in vivo cellular microenvironment. In addition, the fabrication and operation of these multi-organ microsystems are costly and cumbersome, and not suited for high-throughput implementation. These limitations need to be addressed because organ level functions and multi-organ interactions are crucial when evaluating drug toxicity or studying metastasis of tumor cells to specific organs. As a result, many groups including the Rylander team, are investigating methods to create multi organ and tumor systems to gain insight into multi-system response.

4 Conclusion

In vitro models have been invaluable tools for gaining improved understanding of cancer biology and progression. Conventional 2D systems and animal models have provided researchers with a framework upon which to elucidate the basic principles of cancer biology but are limited. Attributes such as relative cost and complexity

have necessitated the development of 3D models to act as a bridge between conventional 2D cell culture systems and animal models. 3D tumor platforms are able to recapitulate the cell-cell and cell-matrix interactions found in vivo. The introduction of microfluidic technology has resulted in the development of advanced 3D tumor platforms that allow researchers to recreate the dynamic tumor niche. Ongoing cancer research utilizes various 3D models such as transwell assays, polymer hydrogels, spheroids, and microfluidic systems and these models vary from group to group in cell type, ECM protein composition, geometry, and fabrication technique. Currently, no one platform can recreate all the dynamic complexities present in the TME such as stromal cells, various gradients, and the immune response. Advancements in the development of more physiologically relevant platforms will provide a deeper understanding of the complex behavior of tumors and uncover new approaches to diagnosis and treatment.

Acknowledgements We would like to acknowledge funding from the National Institute of Health grant 1R21EB019646 that made this work possible.

References

1. Buchanan C, Voigt E, Szot CS, Freeman JW, Vlachos P, Rylander MN (2013) Three-dimensional microfluidic collagen hydrogels for investigating flow-mediated tumor-endothelial signaling and vascular organization. Tissue Eng Part C Methods 20(1):64–75
2. Ingram M, Techy G, Ward B, Imam S, Atkinson R, Ho H, Taylor C (2010) Tissue engineered tumor models. Biotech Histochem 85:213–229
3. Kumar VA, Brewster LP, Caves JM, Chaikof EL (2011) Tissue engineering of blood vessels: functional requirements, progress, and future challenges. Cardiovasc Eng Technol 2:137–148
4. Sung JH, Shuler ML (2012) Microtechnology for mimicking in vivo tissue environment. Ann Biomed Eng 40:1289–1300
5. Abraham LC, Zuena E, Perez-ramirez B, Kaplan DL (2008) Guide to collagen characterization for biomaterial studies. J Biomed Mater Res B Appl Biomater 87:264–285
6. Charulatha V, Rajaram A (2003) Influence of different crosslinking treatments on the physical properties of collagen membranes. Biomaterials 24:759–767
7. Drury JL, Mooney DJ (2003) Hydrogels for tissue engineering: scaffold design variables and applications. Biomaterials 24:4337–4351
8. Kreger S, Bell B, Bailey J, Stites E, Kuske J, Waisner B, Voytik-harbin S (2010) Polymerization and matrix physical properties as important design considerations for soluble collagen formulations. Biopolymers 93:690–707
9. Parenteau-bareil R, Gauvin R, Berthod F (2010) Collagen-based biomaterials for tissue engineering applications. Materials 3:1863–1887
10. Wolf K, Alexander S, Schacht V, Coussens LM, von Andrian UH, van Rheenen J, Deryugina E, Friedl P (2009. Elsevier) Collagen-based cell migration models in vitro and in vivo. Semin Cell Dev Biol 20(8):931–941
11. Yamamura n, Sudo r, Ikeda M, Tanishita K (2007) Effects of the mechanical properties of collagen gel on the in vitro formation of microvessel networks by endothelial cells. Tissue Eng 13:1443–1453
12. Gribova V, Crouzier T, Picart C (2011) A material's point of view on recent developments of polymeric biomaterials: control of mechanical and biochemical properties. J Mater Chem 21:14354–14366

13. Levy-mishali M, Zoldan J, Levenberg S (2009) Effect of scaffold stiffness on myoblast differentiation. Tissue Eng A 15:935–944
14. Ulrich TA, Jain A, Tanner K, Mackay JL, Kumar S (2010) Probing cellular mechanobiology in three-dimensional culture with collagen–agarose matrices. Biomaterials 31:1875–1884
15. Antoine EE, Vlachos PP, Rylander MN (2014) Review of collagen I hydrogels for bioengineered tissue microenvironments: characterization of mechanics, structure, and transport. Tissue Eng Part B Rev 20:683–696
16. Chrobak KM, Potter DR, Tien J (2006) Formation of perfused, functional microvascular tubes in vitro. Microvasc Res 71:185–196
17. Cross VL, Zheng Y, Choi NW, Verbridge SS, Sutermaster BA, Bonassar LJ, Fischbach C, Stroock AD (2010) Dense type I collagen matrices that support cellular remodeling and microfabrication for studies of tumor angiogenesis and vasculogenesis in vitro. Biomaterials 31:8596–8607
18. Koumoutsakos P, Pivkin I, Milde F (2013) The fluid mechanics of cancer and its therapy. Annual review of fluid mechanics 45:325
19. Polacheck WJ, Zervantonakis IK, Kamm RD (2013) Tumor cell migration in complex microenvironments. Cellular and Molecular Life Sciences 70:1335–1356
20. Raub CB, Suresh V, Krasieva T, Lyubovitsky J, Mih JD, Putnam AJ, Tromberg BJ, George SC (2007) Noninvasive assessment of collagen gel microstructure and mechanics using multiphoton microscopy. Biophys J 92:2212–2222
21. Yang Y-L, Motte S, Kaufman LJ (2010) Pore size variable type I collagen gels and their interaction with glioma cells. Biomaterials 31:5678–5688
22. Achilli M, Mantovani D (2010) Tailoring mechanical properties of collagen-based scaffolds for vascular tissue engineering: the effects of pH, temperature and ionic strength on gelation. Polymers 2:664–680
23. Raub CB, Unruh J, Suresh V, Krasieva T, Lindmo T, Gratton E, Tromberg BJ, George SC (2008) Image correlation spectroscopy of multiphoton images correlates with collagen mechanical properties. Biophys J 94:2361–2373
24. Roeder BA, Kokini K, Voytik-harbin SL (2009) Fibril microstructure affects strain transmission within collagen extracellular matrices. J Biomech Eng 131:031004
25. Naciri M, Kuystermans D, Al-rubeai M (2008) Monitoring pH and dissolved oxygen in mammalian cell culture using optical sensors. Cytotechnology 57:245–250
26. Sung KE, Su G, Pehlke C, Trier SM, Eliceiri KW, Keely PJ, Friedl A, Beebe DJ (2009) Control of 3-dimensional collagen matrix polymerization for reproducible human mammary fibroblast cell culture in microfluidic devices. Biomaterials 30:4833–4841
27. Califano JP, Reinhart-king CA (2010) Exogenous and endogenous force regulation of endothelial cell behavior. J Biomech 43:79–86
28. Carey SP, Kraning-rush CM, Williams RM, Reinhart-king CA (2012) Biophysical control of invasive tumor cell behavior by extracellular matrix microarchitecture. Biomaterials 33:4157–4165
29. Ghousifam N, Mortazavian H, Bhowmick R, Vasquez Y, Blum FD, Gappa-fahlenkamp H (2017) A three-dimensional in vitro model to demonstrate the haptotactic effect of monocyte chemoattractant protein-1 on atherosclerosis-associated monocyte migration. Int J Biol Macromol 97:141–147
30. Gunzer M, Friedl P, Niggemann B, Bröcker E-B, Kämpgen E, Zänker KS (2000) Migration of dendritic cells within 3-D collagen lattices is dependent on tissue origin, state of maturation, and matrix structure and is maintained by proinflammatory cytokines. J Leukoc Biol 67:622–629
31. Haugh MG, Murphy CM, Mckiernan RC, Altenbuchner C, O'brien FJ (2011) Crosslinking and mechanical properties significantly influence cell attachment, proliferation, and migration within collagen glycosaminoglycan scaffolds. Tissue Eng A 17:1201–1208
32. Lo C-M, Wang H-B, Dembo M, Wang Y-L (2000) Cell movement is guided by the rigidity of the substrate. Biophys J 79:144–152

33. Provenzano PP, Inman DR, Eliceiri KW, Knittel JG, Yan L, Rueden CT, White JG, Keely PJ (2008) Collagen density promotes mammary tumor initiation and progression. BMC Med 6:11
34. Sieminski A, Hebbel RP, Gooch KJ (2004) The relative magnitudes of endothelial force generation and matrix stiffness modulate capillary morphogenesis in vitro. Exp Cell Res 297:574–584
35. Wells RG (2008) The role of matrix stiffness in regulating cell behavior. Hepatology 47:1394–1400
36. Antoine EE, Vlachos PP, Rylander MN (2015) Tunable collagen I hydrogels for engineered physiological tissue micro-environments. PLoS One 10:e0122500
37. Griffith LG, Swartz MA (2006) Capturing complex 3D tissue physiology in vitro. Nat Rev Mol Cell Biol 7:211–224
38. Horning JL, Sahoo SK, Vijayaraghavalu S, Dimitrijevic S, Vasir JK, Jain TK, Panda AK, Labhasetwar V (2008) 3-D tumor model for in vitro evaluation of anticancer drugs. Mol Pharm 5:849–862
39. Hutmacher DW, Horch RE, Loessner D, Rizzi S, Sieh S, Reichert JC, Clements JA, Beier JP, Arkudas A, Bleiziffer O (2009) Translating tissue engineering technology platforms into cancer research. J Cell Mol Med 13:1417–1427
40. Kim JB (2005. Elsevier) Three-dimensional tissue culture models in cancer biology. Semin Cancer Biol 15(5):365–377
41. Yamada KM, Cukierman E (2007) Modeling tissue morphogenesis and cancer in 3D. Cell 130:601–610
42. Fischbach C, Chen R, Matsumoto T, Schmelzle T, Brugge JS, Polverini PJ, Mooney DJ (2007) Engineering tumors with 3D scaffolds. Nat Methods 4:855–860
43. Ghajar CM, Bissell MJ (2010) Tumor engineering: the other face of tissue engineering. Tissue Eng A 16:2153–2156
44. Hutmacher DW, Loessner D, Rizzi S, Kaplan DL, Mooney DJ, Clements JA (2010) Can tissue engineering concepts advance tumor biology research? Trends Biotechnol 28:125–133
45. Nelson CM, Bissell MJ (2005. Elsevier) Modeling dynamic reciprocity: engineering three-dimensional culture models of breast architecture, function, and neoplastic transformation. Semin Cancer Biol 15(5):342–352
46. Nelson CM, Inman JL, Bissell MJ (2008) Three-dimensional lithographically defined organotypic tissue arrays for quantitative analysis of morphogenesis and neoplastic progression. Nat Protoc 3:674–678
47. Raof NA, Raja WK, Castracane J, Xie Y (2011) Bioengineering embryonic stem cell microenvironments for exploring inhibitory effects on metastatic breast cancer cells. Biomaterials 32:4130–4139
48. Verbridge SS, Choi NW, Zheng Y, Brooks DJ, Stroock AD, Fischbach C (2010) Oxygen-controlled three-dimensional cultures to analyze tumor angiogenesis. Tissue Eng A 16:2133–2141
49. Szot CS, Buchanan CF, Freeman JW, Rylander MN (2011) 3D in vitro bioengineered tumors based on collagen I hydrogels. Biomaterials 32:7905–7912
50. Brahimi-Horn MC, Chiche J, Pouysségur J (2007) Hypoxia and cancer. J Mol Med 85:1301–1307
51. Hanahan D, Weinberg RA (2000) The hallmarks of cancer. cell 100:57–70
52. Kilarski W, Bikfalvi A (2007) Recent developments in tumor angiogenesis. Curr Pharm Biotechnol 8:3–9
53. Zhou J, Schmid T, Schnitzer S, Brüne B (2006) Tumor hypoxia and cancer progression. Cancer Lett 237:10–21
54. Hayes A, Huang W, Yu J, Maisonpierre P, Liu A, Kern F, Lippman M, Mcleskey S, Li L (2000) Expression and function of angiopoietin-1 in breast cancer. Br J Cancer 83:1154
55. Nagata S (2000) Apoptotic DNA fragmentation. Exp Cell Res 256:12–18

56. Bos R, van Diest PJ, de Jong JS, van der Groep P, van der Valk P, van der Wall E (2005) Hypoxia-inducible factor-1α is associated with angiogenesis, and expression of bFGF, PDGF-BB, and EGFR in invasive breast cancer. Histopathology 46:31–36
57. Szot CS, Buchanan CF, Freeman JW, Rylander MN (2013) In vitro angiogenesis induced by tumor-endothelial cell co-culture in bilayered, collagen I hydrogel bioengineered tumors. Tissue Eng Part C Methods 19:864–874
58. Kebers F, Lewalle JM, Desreux J, Munaut C, Devy L, Foidart JM, Noel A (1998) Induction of endothelial cell apoptosis by solid tumor cells. Exp Cell Res 240:197–205
59. Lin RZ, Wang TP, Hung RJ, Chuang YJ, Chien CC, Chang HY (2011) Tumor-induced endothelial cell apoptosis: roles of NAD(P)H oxidase-derived reactive oxygen species. J Cell Physiol 226:1750–1762
60. Mcewen A, Emmanuel C, Medbury H, Leick A, Walker DM, Zoellner H (2003) Induction of contact-dependent endothelial apoptosis by osteosarcoma cells suggests a role for endothelial cell apoptosis in blood-borne metastasis. J Pathol 201:395–403
61. Pepper MS, Ferrara N, Orci L, Montesano R (1992) Potent synergism between vascular endothelial growth factor and basic fibroblast growth factor in the induction of angiogenesis in vitro. Biochem Biophys Res Commun 189:824–831
62. Hong JW, Quake SR (2003) Integrated nanoliter systems. Nat Biotechnol 21:1179–1183
63. Whitesides GM (2006) The origins and the future of microfluidics. Nature 442:368–373
64. Zhang Z, Nagrath S (2013) Microfluidics and cancer: are we there yet? Biomed Microdevices 15:595–609
65. Sung KE, Beebe DJ (2014) Microfluidic 3D models of cancer. Adv Drug Deliv Rev 79-80:68–78
66. Bersini S, Moretti M (2015) 3D functional and perfusable microvascular networks for organotypic microfluidic models. J Mater Sci Mater Med 26:180
67. Xu X, Farach-carson MC, Jia X (2014) Three-dimensional in vitro tumor models for cancer research and drug evaluation. Biotechnol Adv 32:1256–1268
68. Stadler M, Walter S, Walzl A, Kramer N, Unger C, Scherzer M, Unterleuthner D, Hengstschlager M, Krupitza G, Dolznig H (2015) Increased complexity in carcinomas: analyzing and modeling the interaction of human cancer cells with their microenvironment. Semin Cancer Biol 35:107–124
69. Buchanan C, Rylander MN (2013) Microfluidic culture models to study the hydrodynamics of tumor progression and therapeutic response. Biotechnol Bioeng 110:2063–2072
70. Park TH, Shuler ML (2003) Integration of cell culture and microfabrication technology. Biotechnol Prog 19:243–253
71. Buchanan CF, Verbridge SS, Vlachos PP, Rylander MN (2014) Flow shear stress regulates endothelial barrier function and expression of angiogenic factors in a 3D microfluidic tumor vascular model. Cell Adhes Migr 8:517–524
72. Antoine E, Buchanan C, Fezzaa K, Lee WK, Rylander MN, Vlachos P (2013) Flow measurements in a blood-perfused collagen vessel using x-ray micro-particle image velocimetry. PLoS One 8:e81198
73. Garcia-cardena G, Comander J, Anderson KR, Blackman BR, Gimbrone MA Jr (2001) Biomechanical activation of vascular endothelium as a determinant of its functional phenotype. Proc Natl Acad Sci U S A 98:4478–4485
74. Levesque MJ, Nerem RM (1985) The elongation and orientation of cultured endothelial cells in response to shear stress. J Biomech Eng 107:341–347
75. Lin K, Hsu PP, Chen BP, Yuan S, Usami S, Shyy JY, LI YS, Chien S (2000) Molecular mechanism of endothelial growth arrest by laminar shear stress. Proc Natl Acad Sci U S A 97:9385–9389
76. Price GM, Wong KH, Truslow JG, Leung AD, Acharya C, Tien J (2010) Effect of mechanical factors on the function of engineered human blood microvessels in microfluidic collagen gels. Biomaterials 31:6182–6189

77. Song JW, Munn LL (2011) Fluid forces control endothelial sprouting. Proc Natl Acad Sci U S A 108:15342–15347
78. Mitchell MJ, King MR (2013) Fluid Shear Stress Sensitizes Cancer Cells to Receptor-Mediated Apoptosis via Trimeric Death Receptors. New J Phys 15:0150r08
79. Shieh AC, Rozansky HA, Hinz B, Swartz MA (2011) Tumor cell invasion is promoted by interstitial flow-induced matrix priming by stromal fibroblasts. Cancer Res 71:790–800
80. Price GM, Chu KK, Truslow JG, Tang-schomer MD, Golden AP, Mertz J, Tien J (2008) Bonding of macromolecular hydrogels using perturbants. J Am Chem Soc 130:6664–6665
81. Bischel LL, Young EW, Mader BR, Beebe DJ (2013) Tubeless microfluidic angiogenesis assay with three-dimensional endothelial-lined microvessels. Biomaterials 34:1471–1477
82. Zheng Y, Chen J, Craven M, Choi NW, Totorica S, Diaz-Santana A, Kermani P, Hempstead B, Fischbach-teschl C, Lopez JA, Stroock AD (2012) In vitro microvessels for the study of angiogenesis and thrombosis. Proc Natl Acad Sci U S A 109:9342–9347
83. Jeon JS, Bersini S, Gilardi M, Dubini G, Charest JL, Moretti M, Kamm RD (2015) Human 3D vascularized organotypic microfluidic assays to study breast cancer cell extravasation. Proc Natl Acad Sci U S A 112:214–219
84. Vickerman V, Kamm RD (2012) Mechanism of a flow-gated angiogenesis switch: early signaling events at cell-matrix and cell-cell junctions. Integr Biol (Camb) 4:863–874
85. Song JW, Cavnar SP, Walker AC, Luker KE, Gupta M, Tung YC, Luker GD, Takayama S (2009) Microfluidic endothelium for studying the intravascular adhesion of metastatic breast cancer cells. PLoS One 4:e5756
86. Heylman C, Sobrino A, Shirure VS, Hughes CC, George SC (2014) A strategy for integrating essential three-dimensional microphysiological systems of human organs for realistic anticancer drug screening. Exp Biol Med (Maywood) 239:1240–1254
87. Imura Y, Sato K, Yoshimura E (2010) Micro total bioassay system for ingested substances: assessment of intestinal absorption, hepatic metabolism, and bioactivity. Anal Chem 82:9983–9988
88. Sung JH, Kam C, Shuler ML (2010) A microfluidic device for a pharmacokinetic–pharmacodynamic (PK–PD) model on a chip. Lab Chip 10:446–455
89. Zhang C, Zhao Z, Abdul RN, van Noort D, Yu H (2009) Towards a human-on-chip: culturing multiple cell types on a chip with compartmentalized microenvironments. Lab Chip 9:3185